Macromolecular Research, Vol. 17, No. 7, pp 491-498 (2009)

New Semiconducting Multi-branched Conjugated Molecules Bearing 3,4-Ethylenedioxythiophene-based Thiophenyl Moieties for Organic Field Effect Transistor

Dae Chul Kim, Tae Wan Lee, Jung Eun Lee, Kyung Hwan Kim, Min Ju Cho, and Dong Hoon Choi*

Department of Chemistry, Advanced Materials Chemistry Research Center, Korea University, Seoul 136-701, Korea

Yoon Deok Han, Mi Yeon Cho, and Jin-soo Joo

Department of Physics, Korea University, Seoul 136-701, Korea

Received September 29, 2008; Revised November 25, 2008; Accepted November 27, 2008

Abstract: New π-conjugated multi-branched molecules were synthesized through the Horner-Emmons reaction using alkyl-substituted, 3,4-ethylenedioxythiophene-based, thiophenyl aldehydes and octaethyl benzene-1,2,4,5-tetrayltetrakis(methylene) tetraphosphonate as the core unit; these molecules have all been fully characterized. The two multi-branched conjugated molecules exhibited excellent solubility in common organic solvents and good self-film forming properties. The semiconducting properties of these multi-branched molecules were also evaluated in organic field-effect transistors (OFET). With octyltrichlorosilane (OTS) treatment of the surface of the SiO_2 gate insulator, two of the crystalline conjugated molecules, **7** and **8**, exhibited carrier mobilities as high as 2.4 ($\pm$ 0.5)$\times 10^{-3}$ and 1.3 ($\pm$ 0.5)$\times 10^{-3}$ $cm^2V^{-1}s^{-1}$, respectively. The mobility enhancement of OFET by light irradiation (λ = 436 nm) supported the promising photo-controlled switching behavior for the drain current of the device.

Keywords: conjugated semiconductor, multi-branched molecule, mobility, organic field effect transistor, organic phototransistor.

Introduction

Organic semiconductor materials based on extended linear π-conjugated systems have been very intriguing and significant developments have been achieved in these materials over the last several years.[1-3] In the exploration of the application of organic semiconductors in electronic devices, the organic field effect transistor (OFET) is an important component for developing future flexible displays, accompanied by organic light emitting materials.[4-7]

To develop a flexible field effect transistor, α,α'-dialkylsexithiophene and its derivatives have been intensively employed as an active layer material in OFETs.[8-11] However, there is still a lack of sufficient solubility for an efficient solution process.

Compared with the linear organic conjugated oligomers and polymers used in OFETs, multi-branched molecules have a number of advantages, including the ability of a single molecule to demonstrate multi-functionality. The synthesis of π-conjugated multi-branched molecules raises the possibility of creating thiophene derivatives that are fully tethered to the aromatic core, which can be synthesized by a convergent route. Furthermore, the solubility problem in conjugated linear oligothiophene is mostly overcome under a dendritic architecture.[12] Recently, we also demonstrated some soluble star-shaped molecules that showed good solubilities, film forming properties, and reasonably high field effect carrier mobilities.[13]

In the past, the EDOT unit has been employed to improve the conjugative effect and planarity of conjugated thiophene-based oligomeric molecules. Turbiez *et al.*[14] suggested that the analysis of the crystallographic structure of two hybrid quaterthiophenes confirms that the insertion of two adjacent EDOT units in the middle of the molecule leads to a self rigidification of the conjugated systems by intramolecular S···O interactions. We also designed multi-branched molecules bearing ethylenedioxythiophene (EDOT) moieties in the periphery. An improvement in the planarity and conjugation effect could be expected and this can affect the carrier mobility in two star-shaped molecules.

Another interesting feature of the synthesized molecules is the ability to exhibit photosensitivity, to increase the drain current in OFET devices under light irradiation. The control of charge transport properties, including the charge concentration in the active layer of OFETs through both the gate bias and incident light, can lead to an enhanced mobility for OFETs and/or to the development of new types of optoelectronics, such as photo-transistors, photo-controlled memory

*Corresponding Author. E-mail: dhchoi8803@korea.ac.kr

devices, etc.[15,16]

In this study, we prepared crystallizable multi-branched conjugated molecules containing EDOT-based thiophenyl or bithiophenyl moieties as dendritic wedges. We employed the Horner-Emmons method to tether the dendritic wedges to the core, which was free from the transition metal catalyst. Octaethyl benzene-1,2,4,5-tetrayltetrakis(methylene)tetraphosphonate was used as the core unit for the new semiconducting dendritic molecules. We then investigated the optical properties, thermal properties, electrochemical properties, and photophysical properties of the new multi-branched molecules. OFETs based on these molecules were fabricated using a spin-coating method on bare silicon oxide. SiO_2 treated with octyltrichlorosilane (OTS) was also employed to enhance the field effect carrier mobility. They exhibited interesting light harvesting properties and a photosensitivity that could be used to increase the drain current in the phototransistor devices by the irradiation of light. A promising drain current switching behavior was observed, raising the possibility of applying them to optoelectronic memory devices.

Experimental

Synthesis. Compounds **1**, **2**, **3**, and octaethyl benzene-1,2,4,5-tetrayltetrakis(methylene)tetraphosphonate, **6** as a core unit were synthesized by following the method described in the literature, along with a modified method.[17-19]

5-(7-Hexyl-2,3-dihydrothieno[3,4-b][1,4]dioxin-5-yl)thiophene-2-carbaldehyde, 4. A mixture of **1** (4.20 g, 8.13 mmol), **2** (1.85 g, 9.75 mmol), and $[Pd(PPh_3)_4]$ (0.18 g, 0.16 mmol) in dry DMF (50 mL) was heated to 80 °C under argon. After completing the reaction in 24 h, the reaction mixture was cooled to room temperature. After 100 mL of water were added, it was extracted with chloroform. After drying the solution with sodium sulfate, it was concentrated. The resulting crude product was then purified by silica gel column chromatography (eluent; chloroform) to yield 2.29 g (84%) of 5-(7-hexyl-2,3-dihydrothieno[3,4-b][1,4]dioxin-5-yl)thiophene-2-carbaldehyde, **4**.

^{1}H NMR (400 MHz, $CDCl_3$): δ (ppm) 9.85 (s, 1H), 7.66 (d, J = 4.0 Hz, 1H), 7.20 (d, J = 4.0 Hz, 1H), 4.38 (m, 2H), 4.28 (m, 2H), 2.68 (t, J = 7.3 Hz, 2H), 1.59-1.67 (m, 2H), 1.25-1.39 (m, 6H), 0.87 (t, J = 8.0 Hz, 3H).

^{13}C NMR (100 MHz, $CDCl_3$): δ (ppm) 182.69, 145.89, 140.46, 140.22, 138.10, 137.29, 122.23,120.68, 107.54, 66.56, 64.62, 31.72, 30.42, 28.99, 26.16, 22.80, 14.31.

HRMS *m/z* calcd for $C_{17}H_{20}O_3S_2$. [Na]+, 336.08, found 336.10.

5′-(7-Hexyl-2,3-dihydrothieno[3,4-b][1,4]dioxin-5-yl)-2,2′-bithiophene-5-carbaldehyde, 5. The preparation method was the same as that for **4**. Instead of 5-bromothiophene-2-carbaldehyde, **2**, 5′-bromo-2,2′-bithiophene-5-carbaldehyde, **3** was employed. The resulting crude product was then purified by silica gel column chromatography (eluent; chloroform) to yield 0.97 g (80%) of 5′-(7-hexyl-2,3-dihydrothieno[3,4-b][1,4]dioxin-5-yl)-2,2′-bithiophene-5-carbaldehyde, **5**.

^{1}H NMR (400 MHz, $CDCl_3$): δ (ppm) 9.83 (s, 1H), 7.65 (d, J = 4.0 Hz, 1H), 7.25 (d, J = 4.0 Hz, 1H), 7.21 (d, J = 4.0 Hz, 1H), 7.07 (d, J = 4.0 Hz, 1H),), 4.34 (m, 2H), 4.26 (m, 2H), 2.65 (t, J = 8.0 Hz, 2H), 1.58-1.63 (m, 2H), 1.22-1.39 (m, 6H), 0.89 (t, J = 8.0 Hz, 3H).

^{13}C NMR (100 MHz, $CDCl_3$): δ (ppm) 182.52, 147.92, 141.14, 138.60, 137.70, 135.22 133.08, 126.66, 123.55, 128.20, 120.22, 118.20, 107.64, 65.49, 64.69, 31.75, 30.53, 29.02, 26.05, 22.81, 14.32.

HRMS *m/z* calcd for $C_{21}H_{22}O_3S_3$. [Na]+, 418.07, found 418.07.

1,2,4,5-Tetrakis((E)-2-(5-(7-hexyl-2,3-dihydrothieno[3,4-b][1,4]dioxin-5-yl)thiophen-2-yl)vinyl)benzene, 7. An oven dried, mag. stirred, 100 mL of round bottom flask (RBF) was charged with **4** (0.56 g, 1.67 mmol) and **6** (0.27 g, 0.4 mmol) in 50 mL of freshly distilled THF. The reaction was stirred for 0.5 h followed by the addition of potassium *tert*-butoxide (1.12 g, 10.0 mmol). After completing the reaction, the solution was poured into ethanol to collect the precipitates. Purification was performed by reprecipitation into ethanol. Yield 0.33 g (60%).

^{1}H NMR (400 MHz, $CDCl_3$): δ (ppm) 7.65 (s, 2H), 7.21 (d, J = 12.0 Hz, 4H), 7.16 (d, J = 12.0 Hz, 4H), 7.06 (d, J = 3.6 Hz, 4H), 7.01 (d, J = 3.6 Hz, 4H), 4.33 (m, 8H), 4.24 (m, 8H), 2.64 (t, J = 8.0 Hz, 8H), 1.56-1.63 (m, 8H), 1.28-1.39 (m, 24H), 0.89 (t, J = 8.0 Hz, 12H).

^{13}C NMR (100 MHz, $CDCl_3$): δ (ppm) 140.76, 137.99, 137.86, 135.01, 134.88, 127.98, 127.37 124.78, 124.59, 122.61, 117.06, 108.50, 65.39, 64.76, 31.80, 30.63, 29.95, 26.03, 22.85, 14.37.

HRMS *m/z* calcd for $C_{21}H_{22}O_3S_3$. [Na]+, 1406.40, found 1406.37.

1,2,4,5-Tetrakis((E)-2-(5′-(7-hexyl-2,3-dihydrothieno[3,4-b][1,4]dioxin-5-yl)-2,2′-bithiophen-5-yl)vinyl)benzene, 8. The preparation method was the same as that for **7**. Instead of 5-(7-hexyl-2,3-dihydrothieno[3,4-b][1,4]dioxin-5-yl)thiophene-2-carbaldehyde, **4**, 5′-(7-hexyl-2,3-dihydrothieno[3,4-b][1,4]dioxin-5-yl)-2,2′-bithiophene-5-carbaldehyde, **5** was employed. After completing the reaction, the solution was poured into ethanol to collect the precipitates. Yield 0.16 g (65%).

^{1}H NMR (400 MHz, $CDCl_3$): δ (ppm) 7.62 (s, 2H), 7.16 (d, J = 12.0 Hz, 4H), 7.13 (d, J = 12.0 Hz, 4H), 7.09 (d, J = 4.0 Hz, 4H), 7.06 (d, J = 4.0 Hz, 4H), 7.03 (d, J = 4.0 Hz, 4H), 7.00 (d, J = 4.0 Hz, 4H), 4.30 (m, 8H), 4.22 (m, 8H), 2.65 (t, J = 8.0 Hz, 8H), 1.60-1.65 (m, 8H), 1.23-1.39 (m, 24H), 0.91 (t, J = 8.0 Hz, 12H).

^{13}C NMR (100 MHz, $CDCl_3$): δ (ppm) 141.79, 137.90, 137.25, 134.95, 134.86, 133.07, 127.45, 126.78, 124.56, 124.50, 123.66, 123.12 122.80, 122.11, 116.98, 108.24,

65.36, 64.72, 31.71, 30.48, 29.85, 26.03, 22.72, 14.11.

HRMS *m/z* calcd for $C_{21}H_{22}O_3S_3$. [Na]+, 1734.35, found 1735.17.

Instrumental Analysis. The thermal properties were studied in a nitrogen atmosphere on a Mettler DSC 821^e instrument. A thermal gravimetric analysis (TGA) was conducted on a Mettler TGA50 (temperature rate 10 °C/min under N_2). The redox properties of the multi-branched molecules were examined by using cyclic voltammetry (Model: EA161 eDAQ). Thin films were coated on a platinum plate using chloroform as a solvent. The electrolyte solution employed was 0.10 M tetrabutylammonium hexafluorophosphate (Bu_4NPF_6) in a freshly dried MC. Ag/AgCl and Pt wire (0.5 mm in diameter) electrodes were utilized as the reference and counter electrodes, respectively. The scan rate was 50 mV/s. Atomic force microscopy (Digital Instruments Multimode equipped with a nanoscope IIIa controller), operating in a tapping mode with a silicon cantilever, was used to characterize the surface morphologies of the samples. The film samples were fabricated by spin-coating (1,500 rpm) on silicon wafer followed by drying at 70 °C in a vacuum (solvent: chloroform, conc. of the solution: 5 mg/mL).

Absorption and Photoluminescence (PL) Spectroscopy. In order to study the absorption behavior, films of two molecules were fabricated on quartz substrates as follows. The solution (3 wt%) of each molecule in monochlorobenzene was filtered through an acrodisc syringe filter (Millipore 0.2 μm) and subsequently spin-cast on quartz glass. The films were dried overnight at 70 °C for 48 h under vacuum.

Absorption spectra of the samples in the film and solution states (chloroform, conc. 1×10^{-5} mol/L) were obtained using a UV-VIS spectrometer (HP 8453, photodiode array type) in a wavelength range of 190-1,100 nm. PL spectra of the solutions were acquired on a Hitachi F-7000 FL Spectrophotometer.

OFET Fabrication. Bottom-contact OFET devices were fabricated using gold source and drain electrodes, which were thermally evaporated using the conventional method. A p-doped polycrystalline silicon was used as a gate electrode, with a 250 nm bare and surface modified SiO_2 layer used as a gate dielectric insulator. The deposition of a self-assembled monolayer (SAM) with OTS on the SiO_2 gate dielectric was performed by following the method described in the literature.[20]

The gold was deposited onto the untreated and OTS-treated SiO_2 surface via thermal evaporation. A 400 nm thick film of the semiconductor layer was deposited at 25 °C by spin coating a 2 wt% monochlorobenzene solution of the multi-branched molecule. It was then dried and annealed at a specific temperature for 1-0.5 h.

The current-voltage (*I-V*) characteristics of the OFETs using P4TE-H and P4TTE-H molecules were measured under a vacuum below 10^{-2} Torr by using a Keithley 237 SMU. A wire bonder (Kunche & Sona 4524) was used for the electrical path between the Au electrodes and the chip carrier for the OFETs. A mercury-xenon lamp (Spectra-Physics 66902) and monochromator (Newport 77250) were employed for the light source. The optical power was measured by using an optical power meter (Thorlabs PM120) connected to a sensor (Thorlabs S130A).

Results and Discussion

Synthesis. We report here the facile and high-yield synthesis of new p-type EDOT-based multi-branched semiconducting molecules. Scheme I illustrates the synthetic routes for molecules **7** and **8**. These four-armed crystalline multi-branched molecules contain 5-hexyl-7-(5-vinylthiophen-2-yl)-2,3-dihydrotheno[3,4-b][1,4] dioxine or 5-hexyl-7-(5′-vinyl-2,2′-bithiophen-5-yl)-2,3-dihydrotheno[3,4-b][1,4] dioxine as the dendritic wedge, respectively.

5-Bromothiophene-2-carbaldehyde, **2** and 5′-bromo-2,2′-bithiophene-5-carbaldehyde, **3** were prepared by following the method described in the literature.[18,19] Two bromo aldehydes were condensed with tributyl(7-hexyl-2,3-dihydrothieno[3,4-b][1,4]dioxin-5-yl)stannane to yield **4** and **5** via the Stille coupling method.

Horner-Emmons coupling of octaethyl benzene-1,2,4,5-tetrayltetrakis(methylene) tetraphosphonate, **6** and EDOT-thiophene-based carbaldehyde produced the conjugated molecules, **7** and **8**, with a good yield of 60-65%. The resulting material was then purified by silica-gel column chromatography or reprecipitation into ethanol. The identity and purity of the synthetic materials were confirmed by ^1H, ^{13}C NMR, and high resolution mass spetrometer (HRMS). They were found to have good self-film forming properties and were well soluble in various organic solvents, such as chloroform, xylene, MC, chlorobenzene, and THF.

In particular, the solubility of thiophene based multi-branched molecules by inserting an EDOT unit proved to be considerably better than those we reported in the past.[13] The solubility of the synthesized molecule is higher than 2.0 g/100 mL chlorobenzene at RT.

Thermal Analysis. When we employed the EDOT-based thiophenyl multi-branched molecules for OFET applications, their thermal stabilities and dynamic behaviors were emphasized for device fabrication. The thermal properties of **7** and **8** were characterized by differential scanning calorimetry (DSC) and thermogravimetric analysis (TGA). DSC measurement was performed at a heating (cooling) scan rate of 10 (−10) °C/min under nitrogen with the highest temperature limited to below the decomposition temperature. The P4TE-H and P4TTE-H exhibited distinct crystalline-isotropic transitions at 261 and 166 °C, respectively. Exothermic peaks at 184 and 102 °C in P4TE-H and P4TTE-H, respectively, were thought to be cold crystallization temperatures

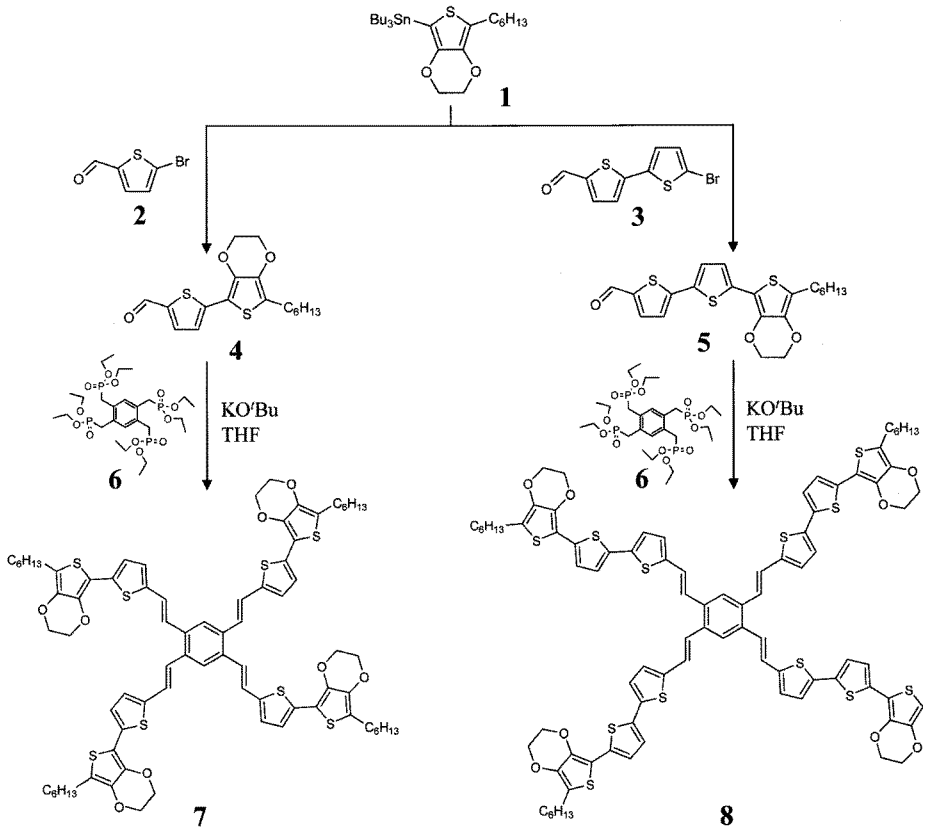

Scheme I. Synthetic procedure for new conjugated multi-branched molecules. P4TE-H, **7** and P4TTE-H, **8**.

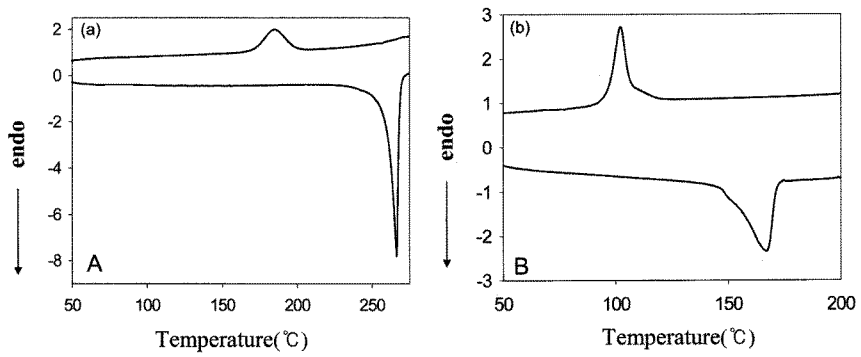

Figure 1. DSC thermograms of two conjugated multi-branched molecules. (a) P4TE-H; (b) P4TTE-H.

(see Figure 1).

TGA measurements at a heating rate of 10 °C/min under nitrogen revealed that **7** and **8** had good thermal stabilities. Compared to the onset decomposition temperature of DH-6T, which is around 309 °C, these crystalline molecules have enhanced onset decomposition temperatures (~381-388 °C).

Optical and Photoluminescence (PL) Properties. Figure 2 shows the absorption and emission spectra for the solutions and thin films of the two molecules. Compared to DH-6T ($CHCl_3$ solution, $\lambda_{abs}^{max} = 438$ nm; $\lambda_{em}^{max} = 517$, 550 nm), the maximum absorption of P4TE-H displayed a blue shift of 7 nm in a solution state, with a value of 431 nm. At

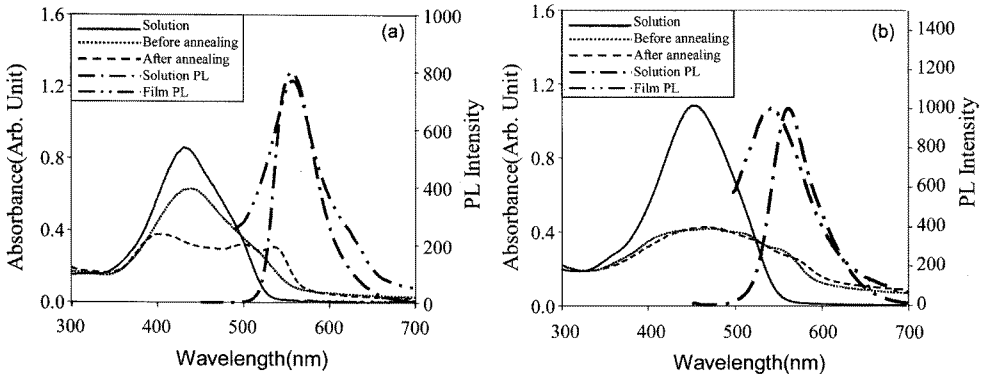

Figure 2. Optical absorption (UV/Vis) and emission (PL) spectra of **P4TE-H** and **P4TTE-H**. *Sample: solution and thin film. (a) **P4TE-H**, excitation wavelength: 420 nm. (b) **P4TTE-H**, excitation wavelength: 420 nm (solution); 440 nm (film).

the same time, P4TTE-H showed a maximum absorbance at 452 nm, which is highly red-shifted. This can be mainly attributed to the longer conjugation length of the molecule.

We observed a drastic spectral change in the film states of **P4TE-H** and **P4TTE-H**, which was attributed to a high degree of intermolecular interaction. For instance, in the **P4TE-H** thin film after annealing at 150 °C, the absorption spectrum was significantly red-shifted, with clear vibronic transitions at 405, 498, and 535 nm, which are attributed to the formation of an ordered structure with intermolecular π-stacking.[12(b),(c),(d)] (see Figure 2(a)).

However, no vibronic absorption peaks were discernible for the **P4TTE-H** thin film, possibly due to the small extent of the intermolecular interaction, and no annealing effect was observed.

The two molecules, **P4TE-H** and **P4TTE-H,** exhibited featureless PL spectral behaviors with emission maxima at 557 and 561 nm in solutions, respectively, as seen in Figure 2. The PL emission maxima showed a bathochromic shift with increasing conjugation lengths. The longer conjugation length in **P4TTE-H** induced a distinct red-shifted emission wavelength.

The PL spectra in solution states revealed a smaller Stokes shift for P4TTE-H (ca. 109 nm) than for P4TE-H (ca. 126 nm) on photoexcitation due to a more rigid ground state geometry, which was consistent with less structural reorganization. In addition, the emission shoulder was observed at 625 nm, which is due to intermolecular interaction. This implies that the close placement of the EDOT and thiophene ring is more effective at enhancing the planarity of the molecules and self-rigidification in **P4TTE-H**.

Properties of OFET Made of Multi-branched Conjugated Molecules. Bottom-contact OFET devices were fabricated using gold source and drain electrodes which were thermally evaporated using the conventional method. P-doped polycrystalline silicon was used as the gate electrode,

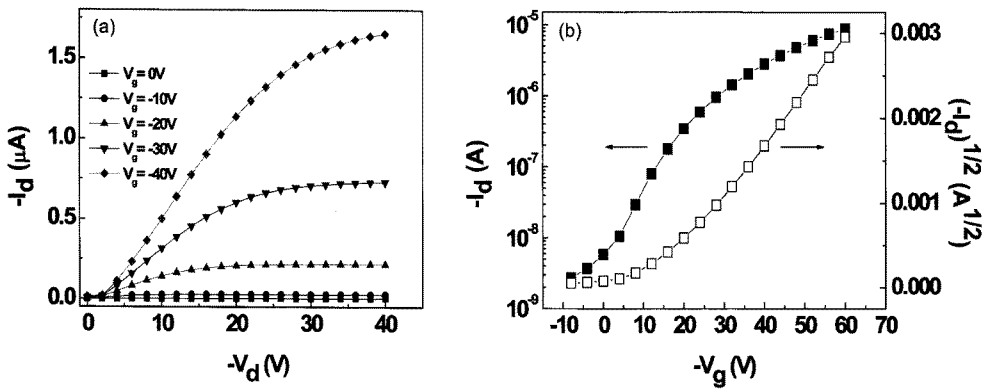

Figure 3. Output (a) and transfer (b) characteristics of OFET made by spin coating of P4TE-H from a monochlorobenzene solution, annealed at 100 °C for 30 min.

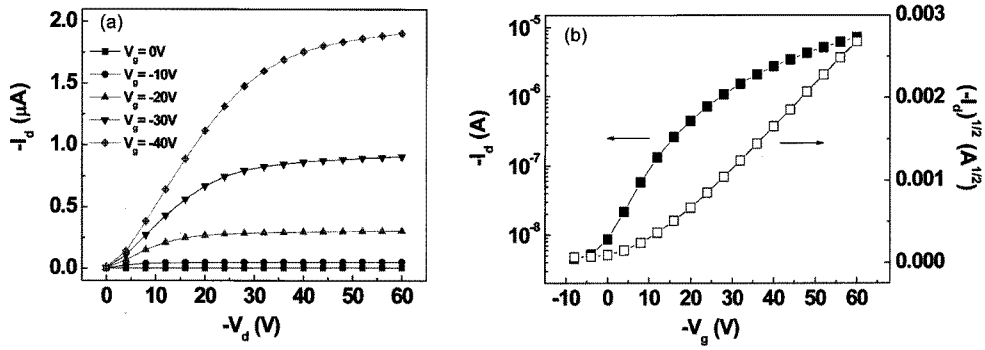

Figure 4. Output (a) and transfer (b) characteristics of OFET made by spin coating of P4TTE-H from a monochlorobenzene solution, annealed at 150 °C for 30 min.

with a 250 nm bare and OTS-treated SiO_2 surface layer used as the gate dielectric insulator. The gold was deposited onto the bare and OTS-treated SiO_2 surface via thermal evaporation.

A 400 nm thin film of the semiconductor was deposited by spin coating a 2 wt% monochlorobenzene solution of the molecules. In order to achieve optimal performance, the **P4TE-H** and **P4TTE-H** OFET devices were further annealed at 150 and 100 °C, respectively, for 30 min.

The output characteristics showed very good saturation behaviors and clear saturation currents that were quadratic to the gate bias (Figures 3 and 4). The field-effect mobilities, μ_{FET}, can be calculated from the amplification characteristics, by using the classical equations describing field-effect transistors.[21] The average mobility values obtained from the measurement of 10 samples are listed in Table I. The transistor devices made from **P4TE-H** and **P4TTE-H** with OTS treated SiO_2 provided field effect average mobilities of 2.4×10^{-3} and 1.3×10^{-3} $cm^2V^{-1}s^{-1}$, respectively, together with current on/off ratio of around 10^3 and low threshold voltages ($V_{th} < -15$ V). The best mobilities for the devices made of **7** and **8** were 2.9×10^{-3} and 1.8×10^{-3} $cm^2V^{-1}s^{-1}$, respectively, which are an order of magnitude higher than those obtained with devices using a bare SiO_2 layer. When using the bare SiO_2 gate insulator, the mobilities were much lower than those with OTS-treated SiO_2 (Table I). The device fabricated with **P4TE-H** exhibited higher carrier mobility, even though the conjugation length was relatively smaller. The intermolecular interaction was clearly evidenced by absorption spectroscopy in the film state. This resulted in a highly efficient carrier transport phenomenon in the device made of **P4TE-H**.

To explain why **7** exhibited the higher mobility, we investigated the surface topography and coverage of the dielectric layer using AFM. In addition to the long-range molecular structural organization, the AFM micrographs display well-resolved surface structures on the dielectric layer. Therefore, we analyzed the topography of the semiconducting layer on the SiO_2 layer. We prepared a solution of each molecule and then performed spin coating to cover the dielectric surface with the respective molecule. After drying and annealing were complete, we took the two micrographs shown in Figure 5.

7 shows a compact surface structure with larger crystallites. **8** is comprised of smaller crystallites than **7**. It can be assumed that the highly packed crystalline molecules on the dielectric layer and the larger size of the crystallites helps the carrier transport by facilitating good connections and transport behavior. The novel multi-branched architecture provides a clear confirmation of the considerable improvement in charge-transport efficiency obtained.

Photo-controlled Properties of Organic Thin Film Transistor. Figure 6(a) compares the source-drain current characteristic curves as a function of gate bias (I_d-V_g) for the **P4TE-H** based OFET devices in dark and light (λ_{ex} = 436 nm, power ≅ 362 μW/cm²) conditions. In this experiment, we used an OTS-treated SiO_2 gate insulator in the TFT device. Typical *p*-type transfer characteristics were observed

Table I. Measured and Calculated Parameters of New Star-shaped Molecules

	T_m (°C)	T_d (°C)	λ_{max}^{abs} (nm)	E_g^{opt} (eV)[a]	λ_{max}^{em} (nm)	Energy Level		μ_{max} (cm^2/Vs)		I_{on}/I_{off}	
						HOMO (eV)	LUMO (eV)	SiO_2	OTS-SiO_2	SiO_2	OTS-SiO_2
P4TE-H	261	381	431	2.17	557	−5.13	−2.96	6.3×10^{-4}	2.4×10^{-3}	$\geq 10^3$	$\geq 10^3$
P4TTE-H	166	388	452	2.02	561	−5.07	−3.05	4.0×10^{-4}	1.3×10^{-3}	$\geq 10^3$	$\geq 10^3$

[a]HOMO-LUMO gap (E_g) measured according to the cutoff wavelength of absorption spectrum ($E_g = 1{,}240/\lambda_{cutoff}$ eV).

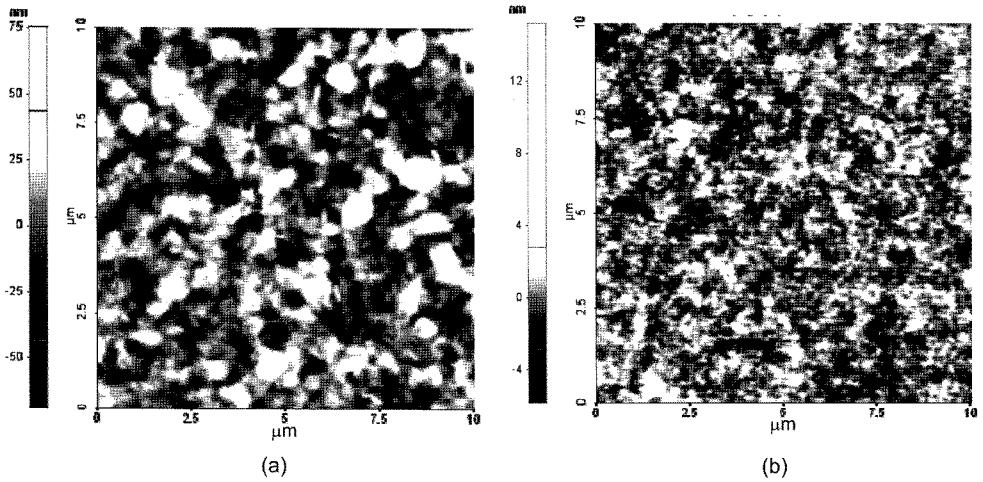

Figure 5. AFM height images (10 μm × 10 μm). (a) P4TE-H, **7**; (b) P4TTE-H, **8**.

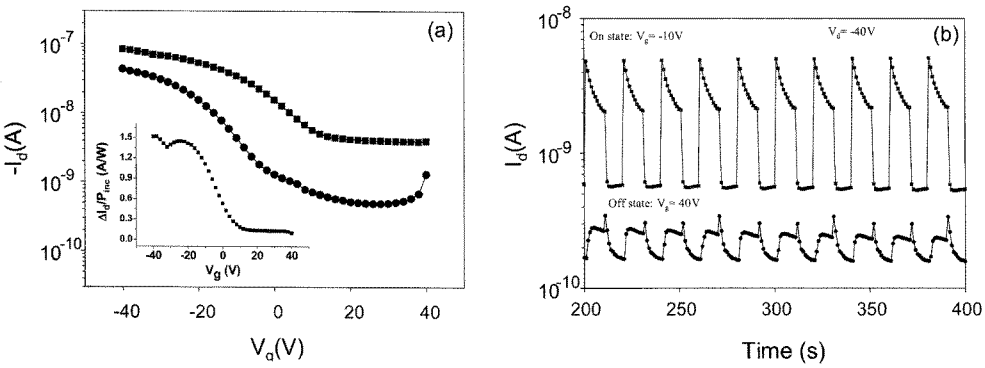

Figure 6. (a) Comparison of I_d-V_g characteristic curves on a logarithmic scale for the y-axis of P4TE-H based OPT devices in dark and light (λ_{ex} = 436 nm, ~361 μW/cm^2) conditions. Inset: Photosensitivity ($\Delta I_d/P_{inc}$) as a function of V_g at V_d = –40 V. (b) Comparison of $I_{on/off}$ switching ratios when applying only V_g and when applying both light (power = 361 μW/cm^2) and V_g (on: V_g = –10 V, off: V_g = 40 V) at V_d = –40 V.

in the dark condition. The charge carrier mobility (μ) and threshold voltage (V_{th}) of the OTFT devices fabricated in this study were estimated to be ~1.7 × 10^{-5} cm^2/Vs and –8.6 V, respectively. The measured I_d increased with the irradiation of a weak intensity of light (λ_{ex}= 436 nm, power ≅ 362 μW/cm^2), as shown in Figure 6(a). When the light was incident on the active layer, bulk conduction in the active layer increased, because trapped charges were excited and delocalized through the efficient absorption of light. Both the charges accumulated in the interface region between the active and dielectric layers through the gate bias (V_g) and the excited charges induced by the light irradiation contributed to the rapid increase of I_d in the active layer. We observed that the I_d of the devices was saturated at ~25 μA at a large negative V_g (< –30 V) with the incident light, which might originate from the traps on the interface and from molecular structures. When irradiating with the light, the off-current (V_g = 0 V) due to bulk conduction rapidly increased, as shown in Figure 6(a). The ratio (I_{ph}/I_{dark}) of the photo-induced current to the dark current was measured to be ~13 at V_g = –2 V, as shown in Figure 6(a). Based on the transfer characteristic curves, we estimated the photo-sensitivity, defined as $\Delta I_d/P_{inc}$, for the OPT devices, where $\Delta I_d \equiv I_{d,ph} - I_{d,dark}$ and P_{inc} is the incident optical power. With a negatively increasing V_g, the photo-sensitivity of the OPT devices using an incident optical power of ~362 μW/cm^2 at λ_{ex} = 436 nm increased up to ~1.5 A/W, as shown in the inset of Figure 6(a).

We obtained a current on/off ($I_{on/off}$) switching performance through the high photo-responsivity of **P4TE-H** based OPTs.

Figure 6(b) compares the $I_{on/off}$ switching performance when applying gate bias only or applying both light (Intensity = 361 μW/cm^2) and gate bias. In order to obtain $I_{on/off}$ switching, gate biases of V_g = −10 V and V_g = 40 V were applied to switch the current on and off, respectively, at a constant drain voltage (V_d = −40 V).

In the light condition, the I_{on} and $I_{on/off}$ switching ratio were measured to be ~4 × 10^{-9} A and ~8.63, respectively, while, in the dark condition, the $I_{on/off}$ switching ratio was ~1.66, as shown in Figure 6(b). The relaxation of drain current during applying V_g = −10 V might be partially due to gradual trapping of photo-induced carriers, which occurs between a dielectric layer and an organic semiconducting (OSC) layer. For the **P4TE-H** based OPTs, the $I_{on/off}$ switching ratio in the light condition was over 5.2 times higher than in the dark condition.

Conclusions

We have successfully synthesized and characterized new EDOT based multi-branched crystalline molecules that are solution processable. They show good film forming properties and a high degree of crystallinity. The intermolecular interaction between the molecules can be tuned by thermal annealing processes, which changes the electronic properties. The large crystallites of **P4TE-H** cover the substrate uniformly and with good network interconnection between the crystallites, which is probably responsible for the moderately high carrier mobility in the solution processed organic semiconductors for OFET. The surface treatment of the SiO_2 dielectric layer enhanced the field-effect mobility and the other device performances. It should be noted that the reproducibility of carrier mobility is significantly better than the materials we have used. When investigating the enhancement of drain current in photo-sensitive organic thin film transistors (OTFTs), we observed the promising switching behavior under alternating device operating conditions. The sensitive photo-controlled OPTs using the **P4TE-H** can be promising for various optoelectronic devices operated with a low intensity of light.

Acknowledgment. This research work was supported by KOSEF (R0120070001128402008) and 21st Century Frontier Research Program (2009). Particularly, M. J. Cho acknowledges the financial support by the Seoul R&BD Program (2008-2009).

References

(1) G. R. Hutchison, M. A. Ranter, and T. J. Marks, *J. Phys. Chem.*, **109**, 3126 (2005).
(2) J. A. Merlo, C. R. Newman, C. P. Gerlach, T. W. Kelley, D. V. Muyres, S. E. Fritz, M. F. Toney, and C. D. Frisbie, *J. Am. Chem. Soc.*, **127**, 3997 (2005).
(3) M. Choi, B. Lim, and J. Jang, *Macromol. Res.*, **16**, 200 (2008).
(4) A. Facchetti, M. H. Yoon, C. L. Stern, G. R. Hutchison, M. A. Ratner, and T. J. Marks, *J. Am. Chem. Soc.*, **126**, 13480 (2004).
(5) A. Md Showkat, K.-P. Lee, and A. I. Gopalan, *Macromol. Res.*, **15**, 575 (2007).
(6) F. J. M. Hoeben, P. Jonkheijm, E. W. Meijer, and A. P. H. Schenning, *Chem. Rev.*, **105**, 1491 (2005).
(7) T. L. Truong, N. D. Luong, and J.-D. Nam, *Macromol. Res.*, **15**, 465 (2007).
(8) H. E. Katz, Z. Bao, and S. L. Gilat, *Acc. Chem. Res.*, **34**, 359 (2001).
(9) Y. Miyata, T. Nishinaga, and K. Komatsu, *J. Org. Chem.*, **70**, 1147 (2005).
(10) A. R. Murphy, J. M. J. Fréchet, P. Chang, J. Lee, and V. Subramanian, *J. Am. Chem. Soc.*, **126**, 1596 (2004).
(11) (a) N. Kiriy, A. Kiriy, V. Bocharova, M. Stamm, S. Richter, M. Plötner, W.-J. Fischer, F. C. Krebs, I. Senkovska, and H.-J. Adler, *Chem. Mater.*, **16**, 4757 (2004); (b) S. Mohapatra, B. T. Holmes, C. R. Newman, C. F. Prendergast, C. D. Frisbie, and M. D. Ward, *Adv. Funct. Mater.*, **14**, 605 (2004).
(12) (a) A. Cravino, S. Roquet, O. Alévêque, P. Leriche, P. Frére, and J. Roncali, *Chem. Mater.*, **18**, 2584 (2006); (b) S. A. Ponomarenko, S. Kirchmeyer, A. Elschner, B.-H. Huisman, A. Karbach, and D. Drechsler, *Adv. Funct. Mater.*, **13**, 591 (2003); (c) Y. Sun, K. Xiao, Y. Liu, J. Wang, J. Pei, G. Yu, and D. Zhu, *Adv. Funct. Mater.*, **15**, 818 (2005); (d) J. Pei, J.-L. Wang, X.-Y. Cao, X.-H. Zhou, and W.-B. Zhang, *J. Am. Chem. Soc.*, **125**, 9944 (2003); (e) S. A. Ponomarenko, E. A. Tatarinova, A. M. Muzafarov, S. Kirchmeyer, L. Brassat, A. Mourran, M. Moeller, S. Setayesh, and D. De Leeuw, *Chem. Mater.*, **18**, 4101 (2006).
(13) K. H. Kim, Z. Chi, M. J. Cho, J.-I. Jin, M. Y. Cho, S. J. Kim, J.-S. Joo, and D. H. Choi, *Chem. Mater.*, **19**, 4925 (2007).
(14) M. Turbiez, P. Fr_re, M. Allain, C. Videlot, J. Ackermann, and J. Roncali, *Chem. Eur. J.*, **11**, 3742 (2005).
(15) Q. Tang, L. Li, Y. Song, Y. Liu, H. Li, W. Xu, Y. Liu, W. Hu, and D. Zhu, *Adv. Mater.*, **19**, 2624 (2007).
(16) S. Dutta and K. S. Narayan, *Adv. Mater.*, **16**, 2151 (2004).
(17) Y. S. Park, D. Kim, H. Lee, and B. Moon, *Org. Lett.*, **8**, 4699 (2006).
(18) Y. Wei, Y. Yang, and J.-M. Yeh, *Chem. Mater.*, **8**, 2659 (1996).
(19) F. Yang, X.-L. Xu, Y.-H. Gong, W.-W. Qiu, Z.-R. Sun, J.-W. Zhou, P. Audebert, and J. Tang, *Tetrahedron*, **63**, 9188 (2007).
(20) D. H. Lee, D. Kim, T. Oh, and K. Cho, *Langmuir*, **20**, 8124 (2004).
(21) J. A. Merlo, C. R. Newman, C. P. Gerlach, T. W. Kelley, D. V. Muyres, S. E. Fritz, M. F. Toney, and C. D. Frisbie, *J. Am. Chem. Soc.*, **127**, 3997 (2005).